

TIROS II RADIATION DATA USERS' MANUAL

SUPPLEMENT

William R. Bandeen

Aeronomy and Meteorology Division  
National Aeronautics and Space Administration  
Goddard Space Flight Center  
Greenbelt, Maryland

May 15, 1962

## FOREWORD

This Supplement pertains to information contained in the *TIROS II Radiation Data Users' Manual* prepared by staff members of the Aeronomy and Meteorology Division, Goddard Space Flight Center, National Aeronautics and Space Administration, and the Meteorological Satellite Laboratory, U. S. Weather Bureau, Department of Commerce, August 15, 1961, and is intended to be used in conjunction with it.

Portions of this Supplement have been taken from an unpublished Meteorological Satellite Laboratory report entitled "A Note on the Quality of Information in the TIROS II Final Meteorological Radiation Tapes" by C. L. Bristor and G. E. Martin whose contributions to these investigations have been extensive and greatly appreciated.

## ABSTRACT

30549

After publication of the *TIROS II Radiation Data Users' Manual* and its companion volume, the *TIROS II Radiation Data Catalog*, additional limitations concerning the usefulness of the data were discovered. This Supplement to the *TIROS II Radiation Data Users' Manual* discusses these additional limitations and elaborates on certain discrepancies originally discussed in the Manual.

In spite of these limitations, much valuable information exists in the TIROS II Final Meteorological Radiation Tapes. A knowledge of these limitations will allow the user to interpret the data properly.

Author

## TABLE OF CONTENTS

	Page
Foreword .....	i
Abstract .....	ii
I. Introduction .....	1
II. Scanning Modes of the TIROS Radiometer .....	1
III. Parameters in the Problem of Data Location .....	3
IV. Timing Errors .....	4
4.1 Errors in the Time Function of the Radiant Emittance Measurements, $\bar{W}(t)$ .....	4
4.1.1 Errors in the End-of-Tape Time, $t_{EOT}$ .....	5
4.1.2 Errors in the Satellite Clock Cycle Count .....	5
4.1.3 Effective Errors in the Satellite Clock Frequency .....	6
4.2 Errors in the Time Function of the Satellite Spin Angle, $\mu(t)$ .....	7
V. Logical Problems in the Computer Program .....	8
5.1 Fixed-Space Rotation of the Principal Line .....	8
5.2 Asymmetrical Single Mode Swaths .....	8
5.3 Alternating Mode Synchronization .....	10
5.4 Extrapolation of Noise on Solar Channels 3 and 5 .....	10
VI. Stereotyped Swath Beginning Response .....	10
VII. Estimate of the Accuracy of the Data .....	10
VIII. Conclusions .....	11
References .....	12
Appendix .....	13

	LIST OF FIGURES	Page
Figure 1	Scanning Modes of the TIROS Radiometer . . . . .	1
Figure 2	Nominal Boundary Nadir Angles for the Different Scanning Modes . . . . .	2
Figure 3	Schematic Illustrating Parameters in the Problem of Data Location . . . . .	3
Figure 4	Geographic Location of Open Mode Data . . . . .	9

	LIST OF TABLES	
Table I	Orbits Having Errors in $t_{EOT}$ . . . . .	5
Table A-I	Orbits Having $\Delta t$ Values of 25 Seconds or More . . . . .	13

## I. INTRODUCTION

The TIROS II meteorological satellite, launched on November 23, 1960, carried the first of a series of five-channel, medium-resolution, scanning radiometers. The *TIROS II Radiation Data Users' Manual* (hereinafter called the "Manual") pointed out a number of limitations of the data from the aspect of utilization.

Since publication of the Manual, considerable research has gone into the entire data reduction system. In this Supplement, we shall elaborate on certain limitations described in the Manual and point out additional limitations of which a potential user should be aware before attempting to interpret the data.

## II. SCANNING MODES OF THE TIROS RADIOMETER

The three possible earth scanning patterns or modes of the TIROS radiometer may be characterized as follows (Figure 1):

- (a) Closed Mode - all scan spots throughout a number of spin cycles of the satellite are earth viewed, either through the "wall" (side) sensor or the "floor" (base-plate) sensor.
- (b) Single Open Mode - some scan spots of a spin cycle are space viewed and the remainder are earth viewed through the wall sensor only or through the floor sensor only.
- (c) Alternating Open Mode - the scan spots of a spin cycle are a combination of space and earth viewed, alternately through the wall sensor and the floor sensor.

In Figure 2 are shown nominal spin (television camera) axis nadir angle values bounding the various radiometer scanning modes. These values are for a height above the earth of about 717 km. From a data processing standpoint, the bounding nadir angle values vary somewhat due to such factors as space contamination in the  $5^\circ$  field of view when the optical axis of the sensor is tangent to the horizon, variations in the height of the satellite, the local earth radius of curvature, the state of the atmosphere at the horizons, any spin axis wobble that may exist,

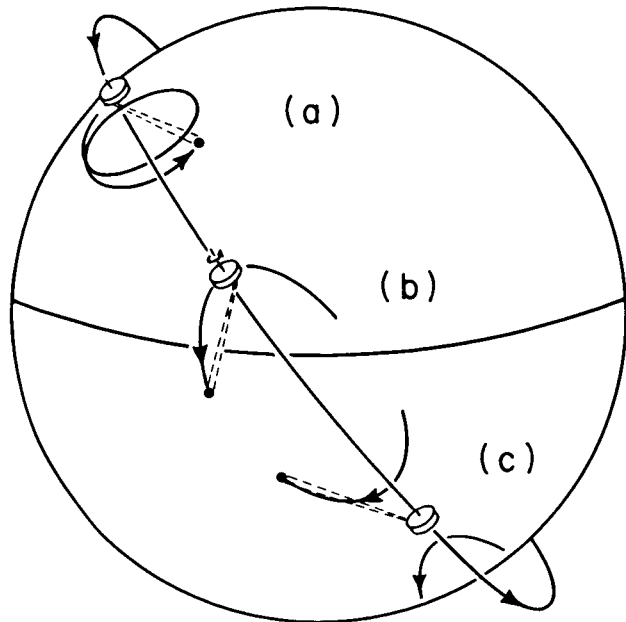


Figure 1—Scanning modes of the TIROS Radiometer: (a) Closed Mode, (b) Single Open Mode, and (c) Alternating Open Mode.

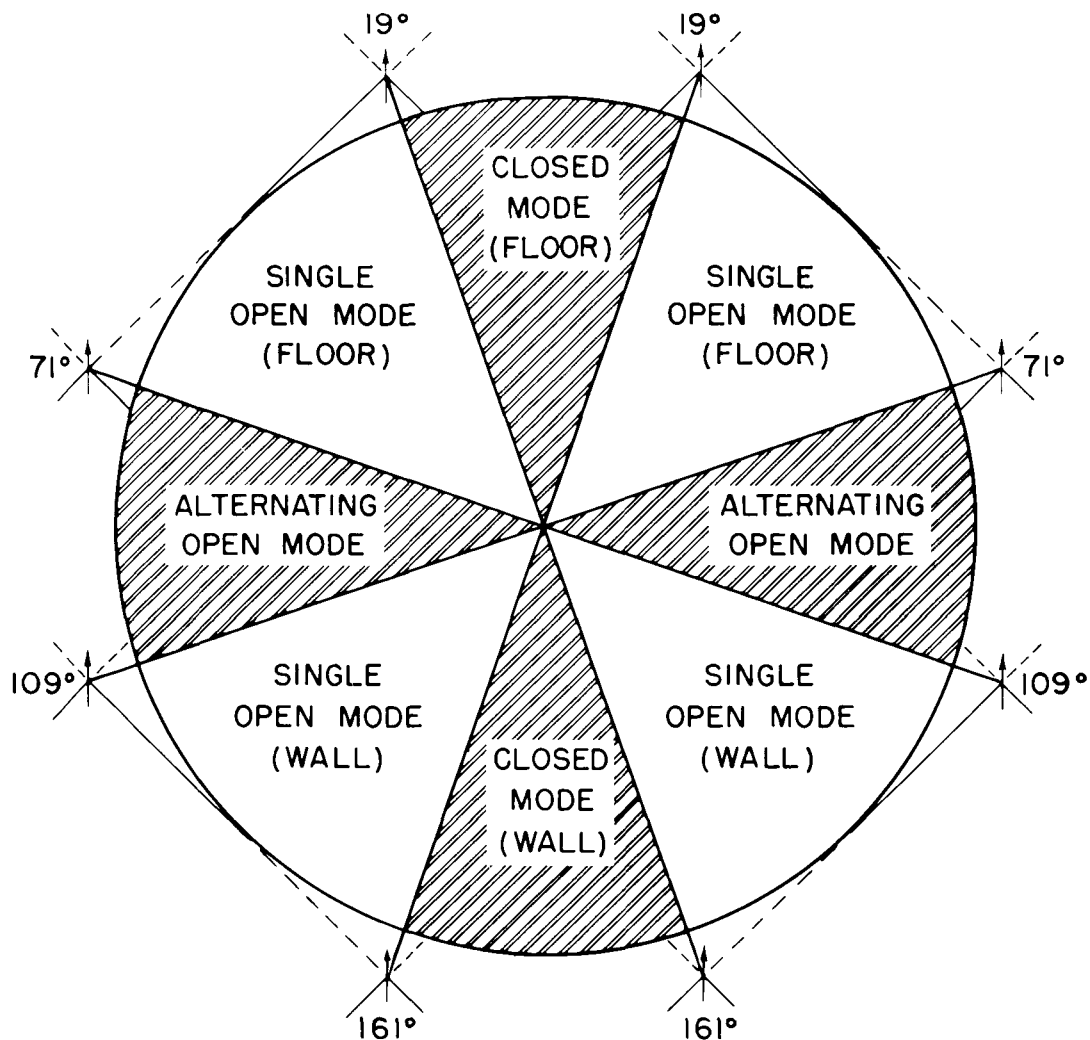


Figure 2—Nominal boundary nadir angles for the different scanning modes at a height of about 717 km. Arrows indicate the spin vector through the top of the satellite, and the nadir angles refer to the opposite direction, viz., the spin (television camera) axis. Solid lines at  $45^\circ$  to the arrows indicate the floor and dashed lines the wall scan of the radiometer.

computer program logic, and the response level which must be somewhat subjectively chosen to discriminate between space and earth viewed spots.

Generally, the minimum nadir angle encountered throughout an orbit is somewhat higher than zero, thus diminishing the periods of closed mode data. In a number of orbits, the minimum nadir angle is greater than  $19^\circ$ , and there are no closed mode data at all.

### III. PARAMETERS IN THE PROBLEM OF DATA LOCATION

The reconstruction of each radiant emittance measurement,  $\bar{W}$ , with its corresponding latitude,  $\theta$ , and longitude,  $\Lambda$ , is a three dimensional manifold which can be expressed, assuming a spherical earth, by (Figure 3)

$$[\bar{W}, \theta, \Lambda] = f[X(t), Y(t), Z(t), G(t), R, \delta, \alpha, \nu, \mu(t), \bar{W}(t)] \quad (1)$$

The position coordinates of the satellite,  $X(t)$ ,  $Y(t)$ ,  $Z(t)$ , are probably known to within two to three kilometers. The Greenwich Hour Angle of the Vernal Equinox,  $G(t)$ , is known very accurately (sidereal time), and the assumed spherical radius of the earth,  $R$ , is taken

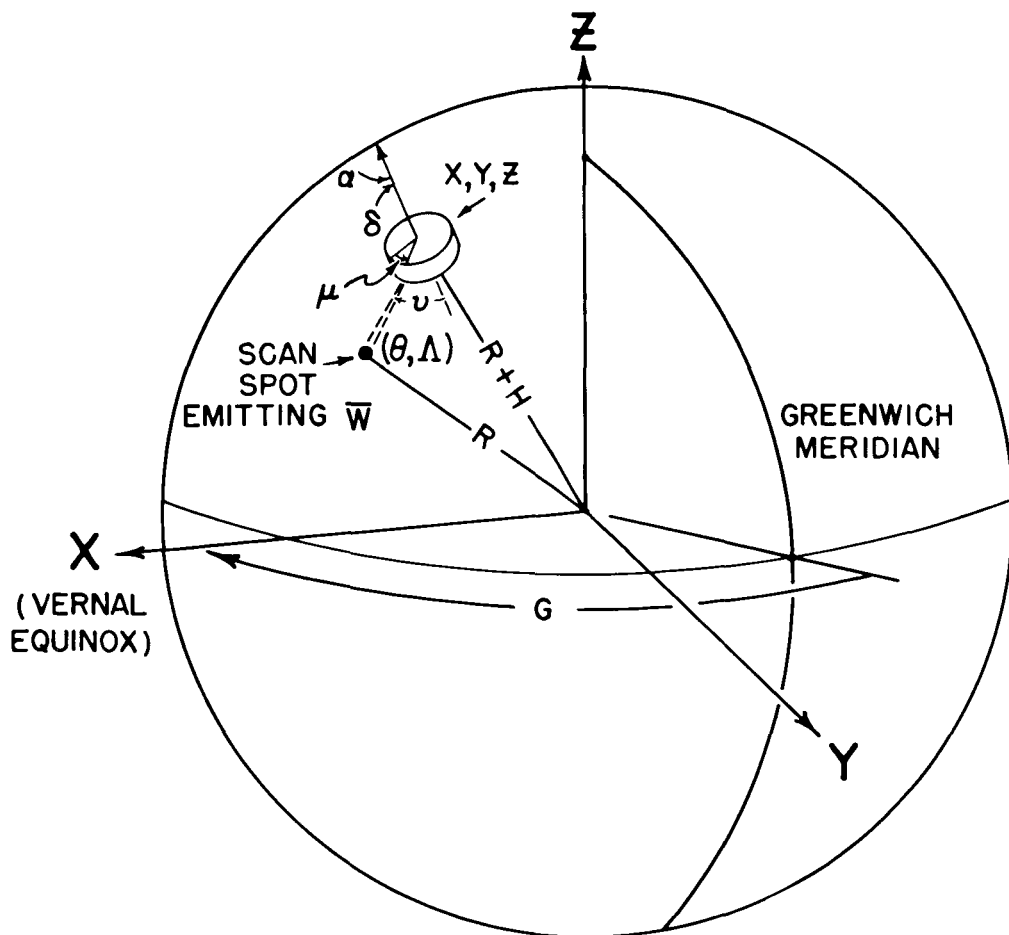


Figure 3—Schematic illustrating parameters in the problem of data location.  $X$ ,  $Y$  and  $Z$  are fixed-space coordinates,  $G$  the Greenwich Hour Angle of the Vernal Equinox,  $R$  the radius of earth,  $\alpha$  and  $\delta$  the right ascension and declination respectively of the spin vector,  $\nu$  the inclination of the radiometer sensors to the spin axis,  $\mu$  the spin angle, and  $\bar{W}$  the radiant emittance measured by a given sensor viewing a particular scan spot identified by latitude  $\theta$ , and longitude  $\Lambda$ . (The fixed-space coordinates of the satellite can alternately be expressed in terms of subsatellite latitude and longitude, the Greenwich hour angle  $G$ , and the height  $H$ .)



as 6371.2 km. The estimated error in spin vector declination,  $\delta$ , and Right Ascension,  $\alpha$ , has been stated in the Manual to be  $2^\circ$  to  $3^\circ$  in great circle arc. A review of attitude data indicates that in rare instances this error might have been as large as  $5^\circ$  or more. Although  $\delta$  and  $\alpha$  are actually slowly varying functions of time, they may be assumed to be constant for a period of the order of an orbit and are so specified in equation (1) for the sake of simplicity (actually this assumption was made in the reduction of the TIROS II data). The precession damper contained within the spacecraft apparently does its job well judging from the clarity of the television pictures and from the smoothness of the track of their principal points over the earth. It is estimated that the angle between the spin axis and the angular momentum vector is less than  $0.5^\circ$ . However, the possibility of a wobble should not be entirely discounted when analyzing the behavior of the data. The inclination of the radiometer optical axes,  $\nu$ , is fixed at a nominal  $45^\circ$  to the spin axis. The field-of-view response surfaces of the individual channels are not strictly symmetrically located about the geometric optical axes. These asymmetries may contribute to an effective deviation from  $45^\circ$  for certain channels. (Generally this effect is believed to be small, but there is evidence that the effective  $\nu$  for channel 5 of the TIROS III radiometer is about  $42.5^\circ$  when viewing through the floor.) However, no conclusive measurements of this type are available for the TIROS II radiometer; hence,  $\nu$  for all channels must be taken as  $45^\circ$ . The two remaining parameters, the time function of the satellite spin angle,  $\mu(t)$ , and the time function of the radiant emittance measurements,  $\bar{W}(t)$ , are the most troublesome in the data location, and, by comparison, errors in all other parameters can probably be neglected.

#### IV. TIMING ERRORS

##### 4.1 Errors in the Time Function of the Radiant Emittance Measurements, $\bar{W}(t)$ .

It is pointed out in Section III of the Manual that reconstruction of the radiation information vitally depends on its correlation with absolute time. The final correlation of the data in time occurs within the computer just before the geographic location of the data is accomplished.

Data time,  $t$ , is calculated by the formula

$$t = t_{\text{EOT}} - n/f \quad (2)$$

where  $t_{\text{EOT}}$  is the absolute time of the "End-of-Tape" (EOT) pulse transmitted from the ground and recorded on the relative clock channel 7 in the satellite. The quantity,  $n$ , is the number of satellite clock cycles counted back from the EOT pulse to a particular data sample, and  $f$  is the frequency of the satellite clock signal. It follows, for example, that if the EOT pulse time is  $11^{\text{h}}40^{\text{m}}10.9^{\text{s}}$ , the number of cycles back to a particular sample is 72,000, and the frequency of the clock is 550 cps, then the absolute time of that particular sample is

$$t = 11^{\text{h}}40^{\text{m}}10.9^{\text{s}} - \frac{72000}{550} = 11^{\text{h}}38^{\text{m}}00^{\text{s}} \quad (3)$$

Differentiating equation (2), the error in absolute time is

$$dt = dt_{\text{EOT}} - \frac{dn}{f} + \frac{n}{f^2} df \quad (4)$$

4.1.1 Errors in the End-of-Tape Time,  $t_{EOT}$ . From equation (4), if the EOT pulse is transmitted to the satellite at a time other than that recorded in the TIROS Control Center Log or if the EOT code word is recorded on the Radiation Data Tape by the Analog-to-Digital Converter at the wrong place, a constant error in time of all data on the tape will result. This type of error was first noticed in orbit 4 on TIROS II FMR Tape reel number 1. In orbit 4, it has been determined that an error at the Data Reduction Center caused the EOT code word to be recorded on the Radiation Data Tape 48 seconds ("real time") too late. Thus, in equation (4),  $dt_{EOT} = -48$  seconds, resulting in the correlation of all data 48 seconds too early (due to this effect alone) and the consequent mislocation of scan spots by moving all data backward along the orbital track. As was pointed out in the Manual, such mislocation does not result merely in translation, but involves distortion of the data as well.

It is believed that this type of error occurred very infrequently, especially after the first two weeks of routine operation after which personnel had become thoroughly trained and operational procedures better established. As far as can be determined, this type of error occurred in only five orbits (Table I), but it has not been possible to survey all data completely and rule out similar occurrences elsewhere. The sense of all such errors was the same (i.e., all data were effectively moved backward along the orbital track).

TABLE I

Orbits Having Errors in  $t_{EOT}$

Readout Orbit Number	$dt_{EOT}$
4	-48 seconds
43	-18 seconds
59	-18 seconds
89	-17 seconds
92	-19 seconds

4.1.2 Errors in the Satellite Clock Cycle Count. In preparing for reduction of the TIROS III data, an error in the Analog-to-Digital converter counter logic was discovered which had been present throughout the processing of the TIROS II data. The nature of this discrepancy was to cause the Analog-to-Digital converter to skip over about one out of every 188 satellite clock cycles. Thus, in equation (4),  $dn \approx -(1/188)n = -0.00532n$ , resulting in the correlation of data too late in time and the consequent mislocation of scan spots by moving all data forward along the orbital track.

The magnitude of this type of error is a function of  $n$  itself, and, hence, ranges from zero at the end of an orbit to

$$-\frac{dn}{f} = -\frac{(-0.00523)(92 \text{ min} \times 60 \text{ sec/min} \times 550 \text{ cps})}{550 \text{ cps}} = +29.4 \text{ sec.} \quad (5)$$

at the beginning of a normal 92-minute data orbit.

4.1.3 Effective Errors in the Satellite Clock Frequency. The time correlation of data in the computer program is accomplished by subtracting the sampling period

$$\frac{72 \text{ clock cycles per sample}}{550 \text{ cps}} = 0.1309099 \text{ sec. per sample} \quad (6)$$

as each data word on the Radiation Data Tape is encountered while counting back from the EOT time to the beginning of the orbit. In a normal orbit, more than 42,000 such subtractions are carried out. After thus time-correlating the data, the computer program marches forward, adding the sampling period as each data word is re-encountered, while at the same time geographically locating the data. This operation is terminated upon reaching the EOT code word. At this point, the resulting computer time,  $t_{\text{EOT}}^*$ , should be equal to the recorded End-of-Tape time,  $t_{\text{EOT}}$ , which was originally read into the computer before reducing the data. However, the difference between these times

$$\Delta t = t_{\text{EOT}}^* - t_{\text{EOT}} \quad (7)$$

in TIROS II was often more than 25 seconds, which corresponds to about 167 km (104 st. miles) displacement along the orbital track.

A cause of the appreciable  $\Delta t$  values apparently involved a precision effect in the computer program, magnified by 42,000 subtractions and an equal number of additions.

No mechanism has been found which consistently explains the observed  $\Delta t$  discrepancies. In the investigation of this effect, a special computer program was written which accomplished 42,000 subtractions of the sampling interval from the EOT time by a floating point "subtract without round" instruction. The effect of this operation was to subtract slightly more than the sampling interval by the amount of the least significant bit in the word representing the total accumulation of time in terms of seconds from 00<sup>h</sup> GMT. For example, for an orbit whose EOT time is 22<sup>h</sup> GMT (79,200 seconds), it follows that the value of the least significant bit in the 27-bit counter containing Greenwich Mean Time in binary form is  $2^{-10}$  (0.0009766) seconds. The effect of subtracting 0.0009766 seconds more than the sampling interval each time can be expressed in terms of an error in clock frequency, viz.,

$$df = \frac{72 \text{ cycles per sample}}{(.130909 + .0009766) \text{ sec. per sample}} - 550 \text{ cps} = -4.072 \text{ cps} \quad (8)$$

From equation (4), it is seen that a time correlation error due to subtracting without rounding would be a function of the cycle count  $n$ , and in this example, considering a normal 92-minute orbit, the error would be

$$\frac{n}{f^2} df = \frac{92 \times 60 \times 550}{(550)^2} (-4.072) = -40.9 \text{ seconds} \quad (9)$$

Because the errors associated with the 42,000 subsequent additions, whether accomplished with or without rounding, were many times smaller than the subtraction errors described above, the time correlation error accumulated by counting back  $n$  cycles from the EOT time should be practically constant throughout the data. From equation (4), the magnitude of this error would be proportional to the length of the orbit (expressed in terms of the maximum cycle count,  $n$ , from the EOT code word to the beginning). Also, when the interrogation of an orbit occurs earlier in the day, it follows that the value of the least significant bit in the 27-bit counter would become smaller (e.g., between 0906 and 1812 GMT it becomes  $2^{-11}$  or 0.0004883 seconds), thus reducing the error in equation (4) for an orbit of the same length.

The computer program used in the TIROS II data reduction, however, utilized a floating point "subtract with round" instruction in accomplishing the subtractions of the sampling interval. In the special computer program written for this investigation, the use of a "subtract with round" instruction resulted in essentially no  $\Delta t$  error after the 42,000 subtractions and subsequent additions. Hence, the exact mechanism causing the observed  $\Delta t$  errors in the TIROS II data is not known, but it is suspected that a precision effect within the computer is involved, which can be equated to an error in clock frequency,  $df$ , in equation (4).

The Appendix contains a list of the 151 orbits which had  $\Delta t$  values of 25 seconds or more. These large discrepancies were all negative and occurred when the End-of-Tape times of the orbits were between 18<sup>h</sup>52<sup>m</sup> GMT and 01<sup>h</sup>59<sup>m</sup> GMT (25<sup>h</sup>59<sup>m</sup> in the computer program). The result of the negative  $\Delta t$  errors is to move the data backward along the orbital track. It is presumed that these timing errors are constant throughout the orbit.

#### 4.2 Errors in the Time Function of the Satellite Spin Angle, $\mu(t)$ .

In practice, one may think in terms of two types of time for the geographic location of data—first "position time" and, secondly, "spin time." Because the geographic location of data is many times more sensitive to spin time than to position time, the two can be treated largely independently. For example, the TIROS track velocity over the earth is about 6.67 km per second; hence, a three-second error in position time would result in a displacement of the data of about 20 km. By contrast, with a spin rate of 10 rpm (60°/sec), a three-second error in spin time could result in a displacement of the data of more than 2400 km!

In the TIROS data reduction, position time is the time calculated within the computer, as previously described. It is initialized only once in an orbit, viz., at the time of the EOT pulse. Spin time, however, is reinitialized every time a horizon is scanned, after which it is counted by means of a previously measured spin rate which is considered to be constant throughout one data orbit (about 92 minutes). In the open modes, spin time is reinitialized about every 6 (or, in the alternating mode, 3) seconds. For a spin rate error of 0.01°/sec, the accrued spin angle error at the end of 6 seconds would be only 0.06°—a negligible amount compared to the 5° field of view of the sensor. However, the closed mode can last for 10 minutes, during which spin time is counted solely by means of the spin rate. Hence, for a spin rate error of 0.01°/sec, the accrued spin angle error at the end of 10 minutes would be 6°, or about equal to one scan spot. Therefore, the spin rate accuracy required in TIROS is 0.01°/sec (or about one part in 6000) for a maximum accrued spin angle error of one scan spot in the closed mode.

The spin rates used in the reduction of the TIROS II data were measured by means of counting cycles of a standard clock at the readout station between sun pulses or pulses from a horizon scanner (corrected for motion in orbit) read out in real time during the interrogation. As described in section 4.1.2, about one out of every 188 satellite clock pulses was skipped in producing the Radiation Data Tape. Therefore, the "mean effective spin rate" for the data should be greater than the actual spin rate by approximately 1/(188). For example, a true spin rate of 56.39°/sec should be increased by  $(.00532)56.39 = 0.3^\circ/\text{sec}$  for data reduction in TIROS II. It follows that at the end of a 10-minute closed mode period, there would be a spin angle error of 180° with corresponding location errors of more than 2400 km!

## V. LOGICAL PROBLEMS IN THE COMPUTER PROGRAM

### 5.1 Fixed-Space Rotation of the Principal Line.

The computer program did not take into account the rotation of the data with reference to the rotation of the principal line (the projection of the local vertical on the image plane) in fixed space. The amount of rotation of the principal line during the closed mode depends primarily on the minimum nadir angle occurring in the orbit and reaches a maximum of  $180^\circ$  when the minimum nadir angle is  $0^\circ$ . This effect contributed to the mislocation of all data in the closed mode.

### 5.2 Asymmetrical Single Mode Swaths.

Since little was known about the pattern of noise before TIROS II radiation data processing began, there was difficulty in building logic into the program to cope with noise in all of its ramifications. In retrospect, one vulnerable decision involves the definition of termination of an earth viewed swath. Under the program rules for TIROS II, a single scan spot response falling below the space-earth discriminant level was sufficient to terminate a swath. This rule seems to have caused large numbers of swaths to be clipped due to noise.

In brief, the program rules operated substantially as follows:

- (a) The population of scan spots above the space-earth discriminant from the first horizon to the second horizon (or a noise spike if one should occur) is symmetrically placed about the principal line (Figure 4).
- (b) The swath population so determined is compared with the theoretical swath size based upon satellite height, nadir angle, and spin rate. If the swath population is smaller than the theoretical swath size, additional spots are added until the theoretical size is reached, and tagged with a minus sign (Figures 4c and 4d).
- (c) If the swath population is larger than the theoretical swath size, the initial off-earth spots are discarded. However, the terminal off-earth spots are retained but tagged with a minus sign (Figure 4e).
- (d) The computer geographically locates every fifth (anchor) spot of a swath, beginning with spot number one. When the program finds an anchor spot off the earth, the swath as it appears on the FMR Tape is terminated. Hence, up to four off-earth spots from (b) or (c) above may be retained on the FMR Tape (Figures 4c, 4d, and 4e).
- (e) Any swath having ten or fewer spots in length is disregarded completely. Such swaths are presumed to be largely adjacent to the horizon and, therefore, vulnerable to space contamination. Hence, this rule provides for three anchor spots in a minimum length swath as specified by the responses. However, faulty attitude (or timing) information may cause some spots to be discarded, leaving these swaths with populations below eleven. Such shorter swaths containing at least two anchor locations still permit location of other spots, but on occasion the swaths have been reduced to less than six, in which event no determination of orientation can be made.

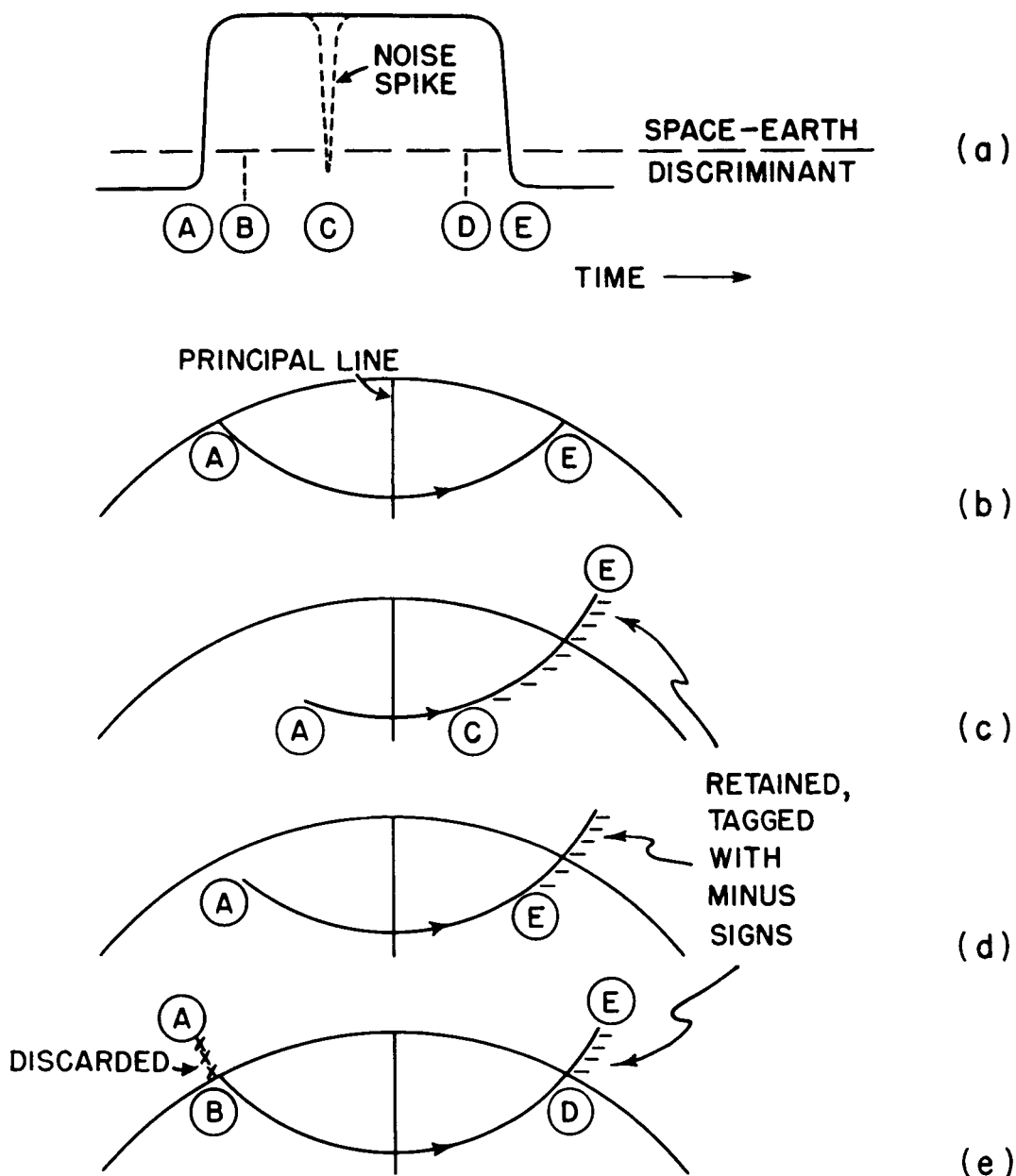


Figure 4—Geographic location of open mode data illustrating (a) the analog signal from a swath, (b) the correct location of the data on earth, (c) the result of a noise spike dropping below the space-earth discriminant, (d) the result of a swath which is shorter than the theoretical length, and (e) the result of a swath which is longer than the theoretical length. Illustrations (d) and (e) are due to attitude or timing errors. The noise spike is not considered in any illustrations except (c).

Hence, noise spikes and/or large attitude (or equivalent timing) errors can be manifested in asymmetrical swaths with their attendant mislocation of data. The nadir angle of the first spot of such swaths (Figures 4c and 4d) is often considerably lower than 60 degrees, thus making their detection relatively easy.

### 5.3 Alternating Mode Synchronization.

The problems of paragraph 5.2 apply equally to the alternating mode. However, the problem of synchronizing the phase of alternation is unique to this type of swath. In the alternating mode, consecutive swaths of data should appear in two different geographic locations as the two sensors (wall, floor) make their forward and backward sweeps—every odd swath being floor and every even swath being wall. However, swaths in this mode often seem to slip out of phase. Obviously, a noise burst which logically changes a larger swath into two shorter swaths will ruin the phase of alternation and cause the data to be erroneously located.

### 5.4 Extrapolation of Noise on Solar Channels 3 and 5.

The signal-to-noise ratio of channel 5 is extremely poor and that of channel 3 (although somewhat better) is also quite poor.

Often under conditions of little or no reflected sunlight, the noise on these channels swings below the calibration zero, and the lower end of the calibration curve is extended by extrapolation to intersect the radiant emittance axis at a large negative number. However, the negative sign is not retained on the FMR Tape. Hence, at nighttime, channel 3 measurements amounting to a large fraction of one diffusely radiated solar constant appear, whereas under similar conditions, channel 5 measurements amounting to several solar constants appear!

Because of poor signal-to-noise ratios, it is recommended that channel 5 data not be used at all and channel 3 data be used only with great caution.

## VI. STEREOTYPED SWATH BEGINNING RESPONSE

A frequent aberration in response has been noted by looking through data produced by a listing code. The calibrated response from all five sensors for the first listed scan spot forms a pattern which appears unrelated to the following responses along the swath. Some of the values in this cluster are obviously unreal. This pattern appears repeatedly on occasion, always with the same stereotyped set of values in the same group of swaths. On other orbits, the stereotyped set of values may be different, but similarly repetitious. There is a suggestion of error in the digital conversion process, but its appearance always as the first response of an affected swath is so far unexplained. An example of such a stereotyped response is shown in a listing on page viii of the *TIROS II Radiation Data Catalog* at the beginning of the third swath, showing values for the five channels respectively of 0.37, 9.37, 967.37, 12.37, and 933.37 watts/m<sup>2</sup>. The false response is contained as part of the FMR Tape data and is not caused by a malfunction of the listing code.

## VII. ESTIMATE OF THE ACCURACY OF THE DATA

### 7.1 Channel 1.

The scaling of the data words on the FMR Tapes provides three binary digits for the fractional part of any radiant emittance measurement (i.e.,  $\bar{W}$  in watts/meter<sup>2</sup>) from

any of the five radiometer channels. Hence, the scaling quantum interval available on the FMR Tapes is  $0.125 \text{ watts/meter}^2$ . This scaling pattern limits the available contrast from the channel 1 data because the entire dynamic range of measurements from this channel is contained in about 14 quantum intervals (i.e., from about  $0.1 \text{ w/m}^2$  to  $1.9 \text{ w/m}^2$ —reference page 18 of the Manual).

Therefore, the contrast in the channel 1 data is low, and the estimated relative accuracy of  $\pm 0.06 \text{ w/m}^2$  ( $\pm 2^\circ \text{ K}$  at  $240^\circ \text{ K}$ ) and the estimated absolute accuracy of  $\pm 0.18 \text{ w/m}^2$  ( $\pm 6^\circ$  at  $240^\circ \text{ K}$ ) in the  $\bar{W}$  measurement is affected appreciably by the scaling quantum interval. For example, the estimated maximum absolute error in  $\bar{W}$  could be  $\pm((0.18 + (1/2)0.125)) = \pm 0.2425 \text{ w/m}^2$  ( $\pm 8^\circ$  at  $240^\circ \text{ K}$ ).

#### 7.2 Channel 2.

The estimated relative accuracy of the channel 2  $\bar{W}$  measurements is  $\pm 1.6 \text{ w/m}^2$  ( $\pm 2^\circ$  at  $270^\circ \text{ K}$ ) and the estimated absolute accuracy is  $\pm 4.0 \text{ w/m}^2$  ( $\pm 5^\circ$  at  $270^\circ \text{ K}$ ).

#### 7.3 Channel 3.

The estimated relative accuracy of the channel 3  $\bar{W}$  measurements is  $\pm 60 \text{ w/m}^2$  under conditions of appreciable reflected sunlight (i.e., about  $1/10$  of a solar constant diffusely reflected, which results in a  $\bar{W}$  measurement of about  $107 \text{ w/m}^2$ , or higher). As explained in paragraph 5.4, the data are unreliable under conditions of little or no reflected sunlight.

In TIROS III, a small though steady decrease in sensitivity of channel 3 was evident from checks made between the time of the original calibration and the launch of the satellite. The cause of this decrease in sensitivity is not fully understood. It is suspected that a similar sensitivity decrease before launch occurred in TIROS II; hence, no estimate of absolute accuracy can be made. However, it is suspected that all channel 3 measurements are somewhat low.

#### 7.4 Channel 4.

The estimated relative accuracy of the channel 4  $\bar{W}$  measurements is  $\pm 1.7 \text{ w/m}^2$  ( $\pm 2^\circ$  at  $260^\circ \text{ K}$ ), and the estimated absolute accuracy is  $\pm 5.0 \text{ w/m}^2$  ( $\pm 6^\circ$  at  $260^\circ \text{ K}$ ).

#### 7.5 Channel 5.

The channel 5 data are considered unreliable (reference paragraph 5.4).

All of the above accuracy estimates, of course, apply only to those time periods before the onset of degradation for each of the channels (reference page 57 of the Manual).

### VIII. CONCLUSIONS

Many somewhat interrelated problems have been discussed and illustrated to demonstrate the quality of TIROS II radiation data from a utilitarian point of view. Despite these remarks, there is still valuable data on the FMR Tapes. With some caution, they may be utilized in devising automated procedures for handling improved future TIROS and Nimbus data and in carrying out limited meteorological studies in order to become better acquainted with the potentialities of such data.



The following recommendations are for those planning user codes which will automatically digest data from the TIROS II FMR Tapes for further processing and analysis (e.g., producing maps).

- (a) Disregard all closed mode data.
- (b) Avoid all single and alternating open mode swaths which are incomplete or skewed because of location problems. These can be detected by low nadir angles accompanying the first spots.
- (c) Avoid alternating open mode swaths where the interlace of floor and wall swaths is erratic.
- (d) Avoid space contamination of data by using a 58 or 60-degree nadir angle acceptance limit.
- (e) Test for and generally avoid all data tagged with a negative sign.
- (f) Avoid all channel 5 data and use channel 3 data with great caution.

It follows that the above restrictions essentially advise mapping or processing only well behaved single mode swaths. Considering the minimum swath length rules for terminating the alternating mode and the fact that any sizeable turning of the spin axis out of the orbital plane may sharply reduce or even eliminate the closed mode altogether, this set of restrictions does not by any means render the data useless. In fact, in many orbits well over half of the data is presented in the long single mode swaths.

Mapping codes described in the *TIROS II Radiation Data Catalog*, plus others developed by the Meteorological Satellite Laboratory, U. S. Weather Bureau, and the Aeronomy and Meteorology Division, Goddard Space Flight Center, are being revised with various options to adapt themselves to faults appearing in the data.

For limited studies where hand plotting of data is possible, some of the data avoided above can be reclaimed.

With all of its imperfections, the data are proving useful in introductory case studies. Correctable faults found in TIROS II data processing are expected to improve greatly the quality of TIROS III data.

## REFERENCES

1. *TIROS II Radiation Data Users' Manual*. NASA, Goddard Space Flight Center, Greenbelt, Maryland, 15 August 1961.
2. *TIROS II Radiation Data Catalog*. NASA, Goddard Space Flight Center, Greenbelt, Maryland, 15 August 1961.

# APPENDIX

Table A-I

Orbits Having  $\Delta t$  Values of 25 Seconds or More  
(Ref. Par. 4.1.3)

Orbit	$\Delta t$ (seconds)	Orbit	$\Delta t$ (seconds)	Orbit	$\Delta t$ (seconds)
390	-28.9	870	-35.5	1562	-37.2
462	-28.4	871	-39.2	1563	-37.6
463	-26.9	872	-38.0	1575	-25.5
476	-32.4	873	-41.2	1576	-28.5
478	-25.9	885	-37.9	1577	-30.3
491	-27.7	886	-38.7	1592	-36.0
492	-25.6	887	-40.6	1604	-26.4
505	-25.4	899	-29.0	1618	-28.8
521	-32.4	900	-34.4	1620	-77.9
550	-27.5	901	-38.3	1621	-36.8
593	-29.4	902	-36.1	1636	-34.8
594	-29.2	958	-27.3	1662	-27.0
595	-28.5	959	-37.7	1665	-23.7
638	-26.2	960	-31.3	1678	-34.0
651	-32.5	973	-34.1	1679	-34.9
652	-36.1	1003	-33.7	1680	-36.3
653	-32.8	1017	-36.5	1706	-35.9
667	-32.9	1061	-36.9	1708	-35.0
694	-27.8	1299	-32.0	1709	-73.3
695	-32.5	1314	-38.1	1710	-36.9
696	-32.4	1343	-33.5	1721	-38.7
710	-31.2	1358	-33.3	1722	-37.0
711	-33.4	1371	-38.1	1723	-38.7
724	-31.9	1386	-36.6	1735	-26.9
725	-27.4	1387	-32.2	1736	-37.3
726	-35.1	1416	-34.2	1737	-34.8
727	-30.7	1429	-35.8	1750	-35.7
739	-35.5	1431	-33.3	1751	-36.3
740	-34.5	1444	-35.3	1752	-38.2
741	-32.6	1445	-34.1	1765	-37.1
782	-32.1	1446	-38.8	1766	-36.3
785	-32.8	1458	-39.8	1779	-28.2
797	-37.8	1459	-37.0	1780	-37.2
798	-36.4	1460	-37.8	1781	-36.4
799	-36.2	1475	-37.4	1794	-38.4
811	-27.2	1487	-35.8	1795	-38.7
812	-37.6	1488	-39.1	1809	-34.6
813	-35.8	1489	-38.4	1823	-29.4
814	-38.7	1502	-30.3	1824	-33.0
815	-36.4	1503	-36.1	1838	-34.4
826	-36.6	1504	-35.0	1855	-33.3
827	-38.9	1517	-38.8	1868	-39.2
828	-38.5	1518	-39.8	1869	-37.2
842	-38.8	1532	-31.9	1882	-34.3
843	-37.8	1533	-36.8	1883	-36.6
844	-36.4	1534	-37.3	1884	-36.0
855	-27.5	1546	-38.0	1926	-34.9
856	-40.2	1547	-39.0	1927	-27.5
857	-38.1	1548	-39.2	1985	-42.3
858	-41.7	1560	-35.2	2043	-31.7
		1561	-31.3		